индекс 3624

ԵՐԵՎԱՆԻ ՖԻԶԻԿԱՅԻ ԻՆՍՏԻՏՈՒՏ
ЕРЕВАНСКИЙ ФИЗИЧЕСКИЙ ИНСТИТУТ

ЕФИ-498(41)-81

G.G.ARAKELIAN, A.A.GRIGORYAN

INCLUSIVE NUCLEON CHARGE EXCHANGE REACTIONS AND OPER MODEL

ԵՐԵՎԱՆ 1981 ЕРЕВАН

ЕФИ-498(41)-81

YEREVAN PHYSICS INSTITUTE

G.G.ARAKELIAN, A.A.GRIGORYAN

INCLUSIVE NUCLEON CHARGE EXCHANGE REACTIONS AND OPER MODEL

Yerevan 1981

Ереванский Физический
ИНСТИТУТ
Зал препринтов

© Ереванский физический институт, 1981

1. Introduction

The reggeized one-pion exchange model (OPER) has been successfully applied to a wide range of exclusive and inclusive processes [1-4]. The inclusive spectra of fast neutrons in pp -collision and of slow protons in pn -collision have been analysed earlier in Ref. [4]. It has been shown that the majority of the experimental data can be described quantitatively in the framework of OPER-model. However the ISR data on the neutron spectra at fixed values of $P_\perp = 0.2 \div 0.8$ GeV/c [5] contradicted the predictions of the model. The model-independent analysis of these spectra was carried out in Ref. [6] where, using the inclusive sum rules, it was shown that the data [5] did not agree with the spectra of other particles also measured at the ISR. The results of later ISR measurements of neutron spectra at $P_\perp = 0$ and $\sqrt{S} = 23 \div 53$ GeV [7] agree with the OPER-model predictions [8].

From this point of view it is interesting to consider the experimental data on the neutron spectra in the reaction

$$pp \to nX \qquad (1)$$

at 12 and 24 GeV/c [9], including the measurements at the same fixed values of $P_\perp$ as in the ISR experiments [5,7]. The present work is devoted to the analysis of the data [9] as well as of the data on the proton spectra in the neutron fragmentation region in the reactions

$$pp \to p_n X \qquad (2)$$

$$\pi^+ n \to p_n X \qquad (3)$$

at momenta 100 and 400 GeV/c [10].

In Sec. 2 the basic formulae for the nucleon spectra in the OPER-model are written down and their brief discussion is given. Sec. 3 deals with the comparison of the OPER-model predictions with the experimental data [9,10] on the reactions (1)-(3). In Sec. 4 on the basis of OPER-model a theoretical analysis of the behaviour of the inclusive nucleon charge exchange reactions at small transverse momenta and $X \to 1$ is carried out.

2. Formulation of the model

The OPER-model has been discussed in much detail in previous works (see e.g. [1-4]) therefore we shall only give the basic formulae for the nucleon spectra in the reactions (1) - (3) and the parametrization of corresponding form factors describing the off mass shell effect of π -meson.

As shown in Refs [3,4] the nucleon spectra in the nucleon fragmentation region in aN -collisions ($a = N, \pi, K \ldots$)

are described by the diagrams shown in Fig. 1. The inclusive cross section corresponding to the diagram 1a has the form

$$\left(E\frac{d\sigma}{d^3p}\right)^a = \frac{G^2_{\pi^0 pp}\cdot|t|}{(2\pi)^3 Q(S,M_N^2,M_a^2)\sqrt{S}}\left|F_1(S,S_1,t)\right|^2\left[Q(S_1,M_a^2,\mu^2)\sqrt{S_1}\,\sigma^{\pi_i a}_{tot}(S_1)\right] \qquad (4)$$

where $S=(P_N+P_a)^2$; $S_1=(P_N+P_a-P)^2$; $t=(P_N-P)^2$; $G^2_{\pi^0 pp}/4\pi = 14.6$;

$Q(x,y,z)=\sqrt{(x-y-z)^2-4yz}/2\sqrt{x}$; M_N, M_a, μ are the mass of nucleon, particle a and π -meson respectively. P_N, P_a - are the momenta of colliding particles, P - is the momentum of the observed nucleon, $\sigma^{\pi_i a}_{tot}$ is the on mass shell total cross section of the i-type pion interaction with the particle a ($\sigma^{\pi^+ p}_{tot}$ in the reaction (1), $\sigma^{\pi^- p}_{tot}$ in the reaction (2), $\sigma^{\pi^+\pi^-}_{tot}$ in the reaction (3)).

The form factor $F_1(S,S_1,t)$ describing the π -meson off mass shell effects in the diagram 1a is parametrized as [1)]

$$F_1(S,S_1,t)=e^{\Lambda_1(t-\mu^2)}\begin{cases}\dfrac{\pi\alpha'_\pi}{2\sin\frac{\pi}{2}\alpha'_\pi(t-\mu^2)} & \text{at } |t|<|t_0| \\ \dfrac{\pi\alpha'_\pi}{2\sin\frac{\pi}{2}\alpha'_\pi(t_0-\mu^2)}\exp\left[R_2^2(t-t_0)\right] & \text{at } |t|>|t_0|\end{cases} \qquad (5)$$

$\Lambda_1 = R_1^2 + \alpha'_\pi \ln S/S_0$; $\alpha'_\pi = 1\ \Gamma\text{эВ}^{-2}$.

The values of the free parameters R_1^2, t_0 and R_2^2 are determined from comparison with experimental data. But in the present work (as distinct from Refs [3,4]) a continuity condition has been imposed on the form factor at the matching

1) The form factor (5) coincides with the one used in Ref. [4] at $|t|<|t_0|$ and differs at $|t|>|t_0|$

point as well as on its first derivative, connecting the parameters R_2^2 and t_o, i.e. only the parameters R_1^2 and t_o remain independent. Their values, found from the comparison with experimental data [9,10] are equal to

$$t_o = -0.7 \text{ GeV/c}^2, \qquad R_1^2 = 0.3 \text{ GeV}^{-2} \tag{6}$$

The corresponding value of R_2^2 is

$$R_2^2 = 0.74 \text{ GeV}^{-2} \tag{6a}$$

The cross section corresponding to the diagram 1b is [4]

$$\left(E\frac{d\sigma}{d^3P}\right)^b = \frac{1}{4\pi^5 Q(S,M_N^2,M_a^2)\sqrt{S}} \int\left[S_2 Q^2(S_2,M_N^2,\mu^2)\frac{d\sigma^i_{CEX}(S_2,t)}{dt}\right] \cdot \tag{7}$$

$$\cdot\left[Q(S_1,M_a^2,\mu^2)\sqrt{S_1}\,\sigma^{\pi i a}_{tot}(S_1)\right]\left|F_2(S,S_1,S_2,t_1)\right|^2 \frac{d^3K}{\omega}$$

where $S_2 = (P+K)^2$, $S_1 = (P_N + P_a - P - K)^2$, $t_1 = (P_N - P - K)^2$

K and ω are the momentum and the energy of the π -meson from the upper block, $d\sigma^i_{CEX}(S_2,t)/dt$ and $\sigma^{\pi i a}_{tot}(S_1)$ are the differential cross section of πN -charge exchange and the total cross section of $\pi i a$ -interaction. The total cross sections of $\pi^0 p$ and $\pi^+ p$ -interactions enter into the formula (7) for the reaction (1), $\sigma^{\pi^0 p}_{tot}$ and $\sigma^{\pi^- p}_{tot}$ for the reaction (2) and $\sigma^{\pi^+\pi^0}_{tot}$ and $\sigma^{\pi^+\pi^-}_{tot}$ for the reaction (3).

The form factor $F_2(S,S_1,S_2,t_1)$ in the formula (7) has the form [1,3]

$$F_2(S,S_1,S_2,t_1) = e^{\Lambda_2(t_1-\mu^2)} \begin{cases} \dfrac{\pi\alpha'_\pi}{2\sin\frac{\pi}{2}\alpha'_\pi(t_1-\mu^2)} & |t_1|<|t_2| \\ \dfrac{\pi\alpha'_\pi}{2\sin\frac{\pi}{2}\alpha'_\pi(t_2-\mu^2)}\exp[R_4^2(t_1-t_2)] & |t_1|>|t_2| \end{cases} \tag{8}$$

$$\Lambda_2 = R_3^2 + \alpha'_\pi \ln\frac{S(K_\perp^2+\mu^2)}{S_1 S_2}$$

where $K_\perp$ is the transverse momentum of the pion from the upper block.

An additional threshold factor

$$f_\Delta = q_t/q_o \cdot \exp\left[R_\Delta^2(t-\mu^2)\right]$$

$$q_t = Q(S_2, M_N^2, t); \quad q_o = Q(S_2, M_N^2, \mu^2)$$

is introduced into the P -wave charge exchange amplitude (where the contribution of Δ -isobar dominates).

The values of the parameters R_3^2, R_4^2, t_2 and R_Δ^2 have been taken from Refs [3,4] and are equal to: $t_2 = -0.4$ GeV^2, $R_3^2 = 0.5$ GeV^{-2}, $R_4^2 = 3.5$ GeV^{-2}, $R_\Delta^2 = 2.75$ GeV^{-2}.

The diagram 1c contains no vacuum exchange and at the considered energies its contribution is negligible.

It should be noted that in the considered model the π -meson exchange is understood in some generalized sense since the model describes the data at large values of $|t|$ where other exchanges, absorption corrections etc. become essential. A part of these effects is taken into account with the help of form factors. In this connection one should talk about the exchange of "effective" π -mesons, meaning a hadron system whose interaction at small $|t|$ is well approximated by the pion exchange. It is important that the π -meson exchange allows one to determine the absolute normalization of cross sections at small $|t|$, while the behaviour at large values of $|t|$ is determined by the form factors.

3. Discussion of results

In this section we shall compare the OPER-model predictions with experimental data [9,10] on the reactions (1)-(3) and discuss briefly the results.

As it has been pointed out, the difference between the cross sections of the reactions (1)-(3) in OPER-model is determined by the difference of total cross sections in the lower block of diagrams 1a,b ($\sigma_{tot}^{\pi^+p}(S_1)$ and $\sigma_{tot}^{\pi^-p}(S_1)$ in the reactions (1) and (2), $\sigma_{tot}^{\pi^+\pi^+}(S_1)$ in the reaction (3)). This difference is the largest in the resonance region. At low initial energies the theoretical curves have a structure which is connected with the resonance contribution to the total cross section of πa -scattering in the lower block of diagram 1a. With the rise of energy the resonance region contribution, having a nonscaling character, tends to $X \simeq 1$ ($1-X_0 \simeq \frac{M_0^2}{S}$ M_0 is the resonance mass), and the area under the resonance peak decreases like $1/S^2$ (because of the π -meson exchange). Therefore at large energies the structure connected with the resonance region is practically not seen. The resonance structure connected with the total cross section $\sigma_{tot}^{\pi a}$ in the lower block of the diagram 1b is smeared due to the integration over the momentum of π -meson in the upper block. The corresponding region of the variable X also tends to $X \simeq 1$ with the rise of initial energy, and the area under the peak decreases, like $1/S$ (due to the ρ -meson exchange in the upper block). The earlier data at the initial momenta (P_L = 10 + 100 GeV/c) have had resolutions insuffi-

cient to clear up this structure (see e.g. [3,4]). However new data on the neutron spectra in the reaction (1) at P_L = 12 and 24 GeV/c [9] confirm the model predictions.

In Figs 2a,b the comparison of the theoretical calculations with the experimental data on the dependence of the nucleon invariant spectra in the reaction (1) on the scaling variable X at fixed values of $P_\perp$ is presented. The X - distribution at small fixed $P_\perp$ shows a maximum at $X \sim 0.8$. In OPER-model such a behaviour has kinematic character and is connected with the exponential dependence of the form factor on t (at fixed $P_\perp$ the t increases with the decrease of X). The resonance peak height (Δ^{++} in the diagram 1a for the reaction (1)) decreases with the rise of $P_\perp$ as well. As seen on Fig. 2 the form of spectrum measured in the experiment [9] coincides with the OPER-model predictions as distinct from the data [5] at the ISR energies. A detailed analysis of the data [5] has been carried out in the Ref. [6] therefore we shall only compare here the results of the experiments at the value of $P_\perp$ = 0.2 GeV/c (Fig. 3). The solid curve in Fig. 3 is calculated at P_L = 24 GeV/c, the dashed one - at $\sqrt{S}$ = 53 GeV.

Fig. 4 shows the dependence on X of the neutron invariant spectra (reaction (1)) integrated over transverse momentum [5] . The solid curve corresponds to the calculations at P_L = 12 GeV/c, the dotted one - at 24 GeV/c.

In Fig. 5 the dependence of the cross section $\frac{S}{\pi} d\sigma/dt dM^2$ on M^2/S is presented, and in Fig. 6 - the dependence of $E\frac{d\sigma}{d^3p}$ on the variable $X = 1 - M^2/S$ at various fixed va-

lues of $|t|$ ($M^2 \equiv S_1$ - is the missing mass). The structure at small values of M^2/S in Fig. 5 (of large X in Fig. 6), decreasing with the rise of $|t|$, is connected, as already mentioned, with the contribution of resonances to the $\pi^+ p$-total cross section in the diagram 1a.

Experimental data [10] on the cross sections $S\,d\sigma/dM^2$ (Fig. 7) and $d\sigma/dt$ (Fig. 9) of the reactions (2) and (3) at P_L = 100 and 400 GeV/c are obtained from the scattering of p and π^+-beams in the deuterium bubble chamber. The fact that the cross section $S\,d\sigma/dM^2$ equals to zero at $M^2/S > 0.6$ in Fig. 7 is due to the experimental kinematical restriction on the momentum of detected protons leading to the limitation on $|t| < 1$ GeV/c [2]. The solid curve in Figs 7 and 8 corresponds to the reaction (2) at P_L = 400 GeV/c, the dotted one - to the reaction (3) at 100 GeV/c. The calculations of cross sections for the reaction (2) at 100 GeV/c slightly differ from the given curve.

The extraction of data on the scattering on neutron requires the consideration of Fermi motion in deuteron. The presence of experimental points in the nonphysical region ($M^2/S < 0$, see Fig. 7) testifies to the fact that this effect has not been considered with sufficient accuracy. A more thorough consideration of Fermi motion should in principle improve the agreement with theoretical predictions.

Thus the OPER-model with the form factors (5), (6) and (8) describes the majority of considered experimental data [9,10] with an accuracy 20-30%.

4. Nucleon charge exchange spectra at large X and small $P_\perp$.

In this section we shall discuss in the framework of OPER-model the behaviour of inclusive nucleon charge exchange reaction near the kinematic region boundary ($X \to 1$, small $P_\perp$).

In the asymptotic region ($S, S_1, S_2 \gg M_N^2$) the contributions of the diagram 1a,b have the well-known triple-Regge form [4] ($\pi\pi\mathbb{P}$ and $\rho\rho\mathbb{P}$ respectively). The OPER-model makes it possible to calculate the triple-Regge contributions in absolute normalization and allows to determine the region of X where the $\rho\rho\mathbb{P}$-vertex dominates. The possibility of separating the $\rho\rho\mathbb{P}$-mechanism contribution (large S_2 on the diagram 1b) from the Δ-isobar one is also essential. The quantitaive calculations given below show that the $\rho\rho\mathbb{P}$-mechanism contribution prevails only at $X \gtrsim 0.99$ (a standard phenomenological triple-Regge analysis is normally carried out already for $X > 0.8$).

In the triple-Regge region the contribution of the diagram 1a ($\pi\pi\mathbb{P}$, see Fig. 9a) to the spectra of particles in the reactions (1)-(3) has the form

$$\left(E\frac{d\sigma}{d^3p}\right)^a_{\pi\pi\mathbb{P}} \equiv \rho^a_{\pi\pi\mathbb{P}} = \frac{|t|}{(|t|+\mu^2)^2}(1-x)^{1-2\alpha_\pi(t)}\,\phi^a(t) \qquad (10)$$

The triple-Regge asymptotics $\rho\rho\mathbb{P}$ (Fig. 9b) which corresponds to the diagram 1b has the form

$$\left(E\frac{d\sigma}{d^3p}\right)^b_{\rho\rho\mathbb{P}} \equiv \rho^b_{\rho\rho\mathbb{P}} = (1-x)^{1-2\alpha_\rho(t)}\,\phi^b(t) \qquad (11)$$

For the reactions (1) and (2) the kinematic variables X, $P_\perp$ and t satisfy asymptotically ($S \gg M_N^2$) the relation

$$t = -\frac{P_\perp^2}{X} - \frac{(1-X)}{X} M_N^2 \qquad (12)$$

Let us consider the behaviour of the asymptotics (10) and (11) at $X \to 1$.

Diagram 1a (9a)

As far as in this region the function $\phi^a(t)$ smoothly depends on X and $P_\perp$, it follows from (10) that at large X and small $P_\perp$ the behaviour of the diagram 1a(9a) contribution is determined by the π-meson factor

$$\frac{|t|}{(|t|+\mu^2)^2}\,(1-X)^{1-2\alpha_\pi(t)} \qquad (13)$$

The substitution of (12) into (13) leads to the expression

$$\frac{\frac{P_\perp^2}{X} + \frac{(1-X)^2}{X} M_N^2}{\left(\frac{P_\perp^2}{X} + \frac{(1-X)^2}{X} M_N^2 + \mu^2\right)^2}\,(1-X)^{1-2\alpha_\pi\left(\frac{P_\perp^2}{X} + \frac{(1-X)^2}{X} M_N^2\right)} \qquad (14)$$

It is seen from (14) that the behaviour versus X depends essentially on the value of transverse momentum $P_\perp$.

a) $P_\perp = 0$.

In this case it follows from (14) that at $X \to 1$

$$\rho^a_{\pi\pi\mathbb{P}}(P_\perp = 0) \sim \frac{(1-X)^{3-2\alpha_\pi(t_{min})}}{[(1-X)^2 M_N^2 + \mu^2]^2} \qquad (15)$$

where $t_{min} = -\frac{(1-X)^2}{X} M_N^2$

From (15) it is seen that if $(1-x) < \frac{\mu}{M_N} \simeq 0.15$ then

$$\rho^a_{\pi\pi\mathbb{P}}(P_\perp = 0) \sim (1-x)^{3-2\alpha_\pi(t_{min})} \simeq (1-x)^3 \qquad (16a)$$

and if $(1-x) > \frac{\mu}{M_N}$ then

$$\rho^a_{\pi\pi\mathbb{P}}(P_\perp = 0) \sim (1-x)^{-1-2\alpha_\pi(t_{min})} \qquad (16b)$$

The contribution of diagram 1a calculated at $\sqrt{S} = 53$ GeV and $P_\perp = 0$ is presented in Fig. 10 by a dashed line.

b) the case of $P_\perp \neq 0$.

In this case the behaviour of ρ^a at very small values of $(1-x)$ sharply differs from the case of $P_\perp = 0$. For instance, if $(1-x) < \frac{P_\perp}{M_N}$ then

$$\rho^a_{\pi\pi\mathbb{P}} \sim (1-x)^{1-2\alpha_\pi(t)}$$

Diagram 1b(9b)

Consider now the contribution of diagram 1b (the dot-dashed line in Fig. 10 shows the result of calculations at $P_\perp = 0$ and $\sqrt{S} = 53$ GeV). As distinct from the diagram 1a the triple-Regge asymptotics ($\rho\rho\mathbb{P}$) for this diagram is valid at very large $X > X_0$ only. As shown in Ref. [3] at smaller $X < X_0$ the contribution of the resonance ($S_2 < 4\text{GeV}^2$) region of the charge exchange reaction dominates.

As seen from Fig. 10 in our case ($P_\perp = 0$) the asymptotic regime ($\rho\rho\mathbb{P}$)

$$\rho^b_{\rho\rho\mathbb{P}} \sim (1-x)^{1-2\alpha_\rho(t_{min})} \simeq \text{const}$$

begins at $X \simeq 0.99$. Thus the particle spectra in the reac-

tions (1) and (2) must be constant at $P_\perp = 0$ and $X > 0.9$ since the diagram 1b contribution dominates in this region. The summary contribution of the diagrams 1a and 1b is shown in Fig. 10 by a solid line which shows that the behaviour of spectra in inclusive nucleon charge exchange reactions is determined not only by the π -meson contribution.

Thus the above analysis shows that the measurements of inclusive nucleon charge exchange reactions in the region of very small $(1 - x)$ and fixed $P_\perp$ (beginning with $P_\perp = 0$) are of great interest for checking the model predictions and extracting various triple-Regge contributions.

The authors would like to thank K.G.Boreskov for his permanent interest in the work and critical remarks and A.B.Kaidalov for useful discussions.

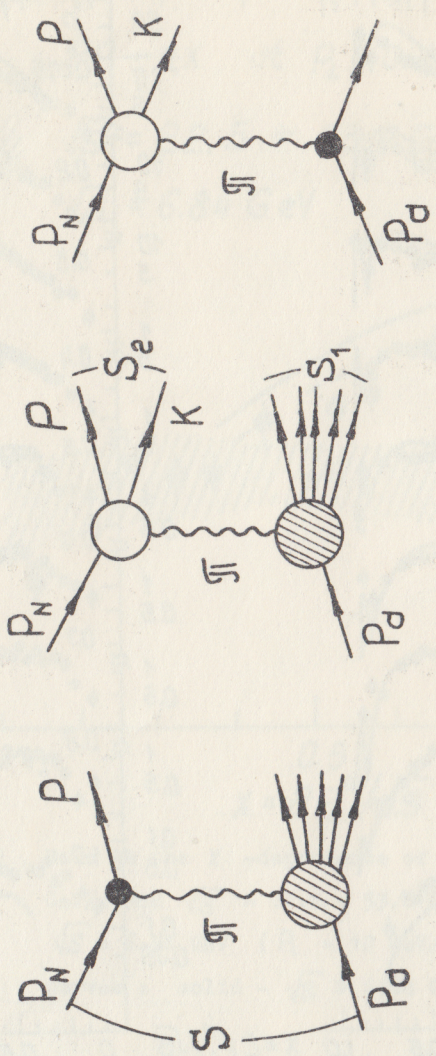


Fig. 1 Diagrams of one-pion exchange for the nucleon spectra.

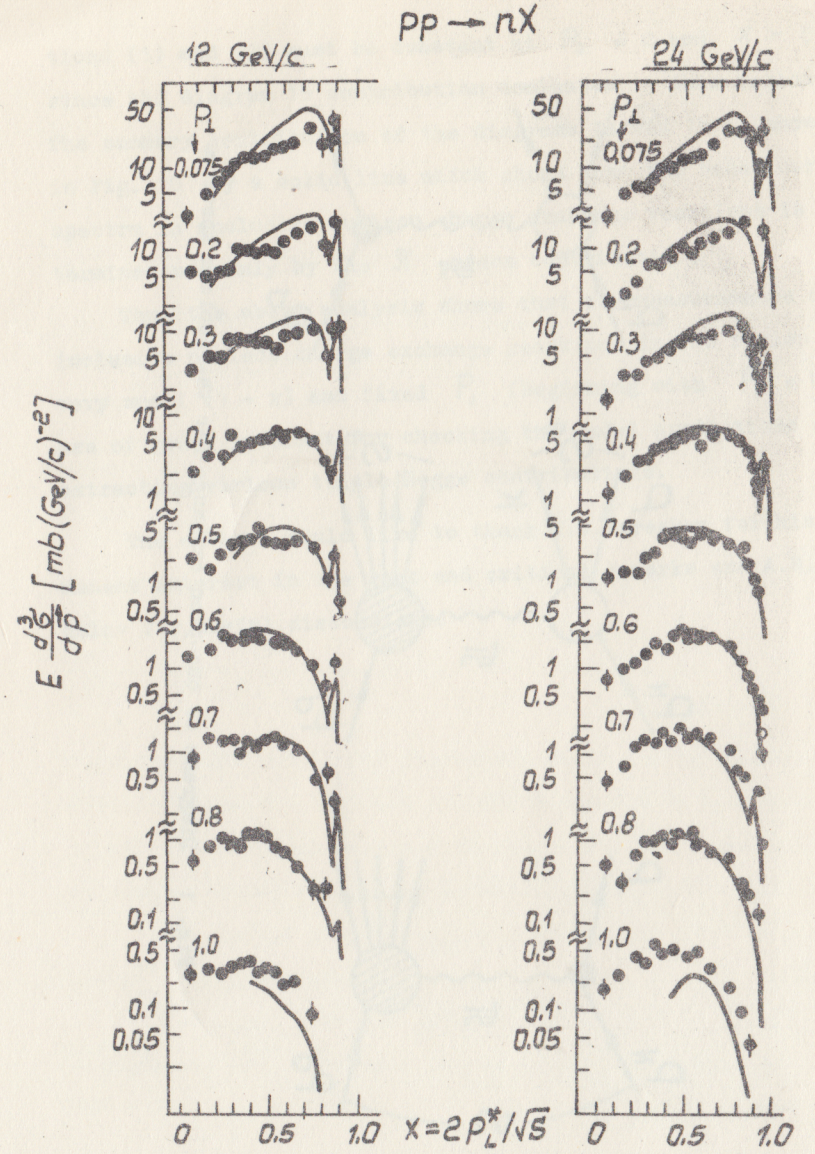


Fig. 2 Comparison of theoretical calculations with experimental data for the dependence of $E\frac{d\sigma}{d^3p}$ on X for the reaction (1); a) P_L = 12 GeV/c, b) P_L =24 GeV/c at fixed transverse momenta $P_\perp$ [9].

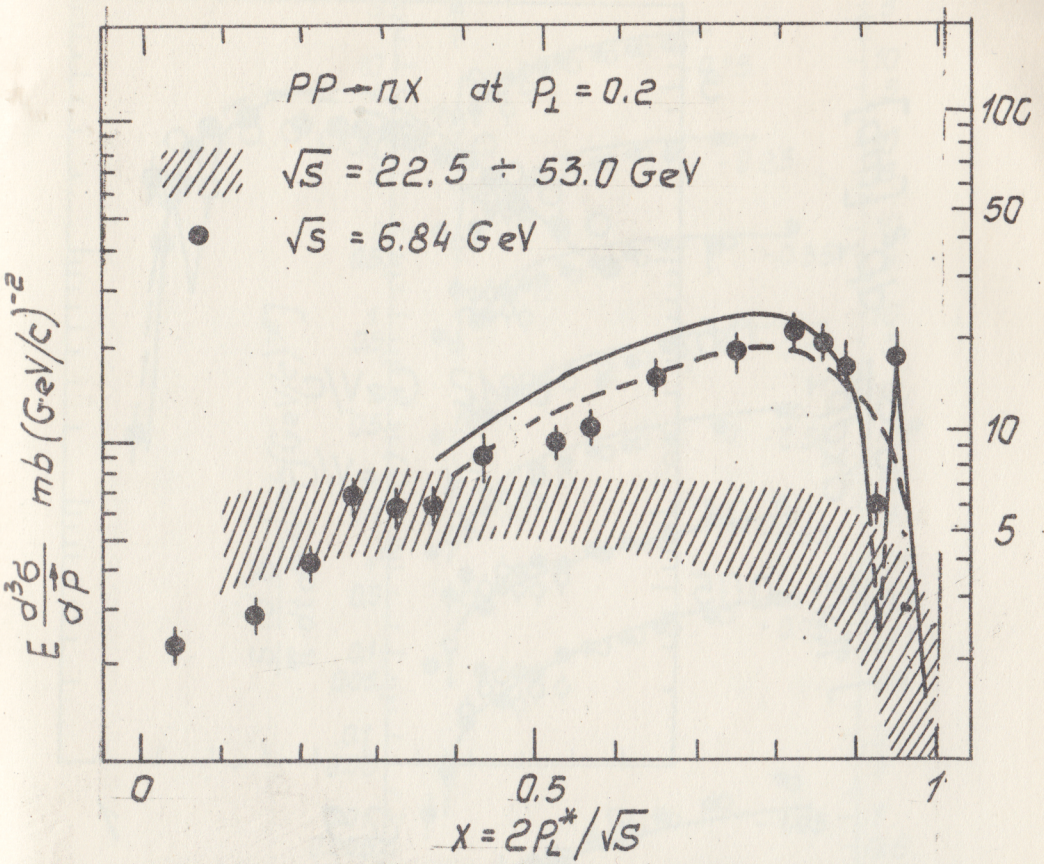


Fig. 3 Data on the X -dependence of $E\frac{d\sigma}{d^3p}$ at $P_\perp$ = 0.2 GeV/c and $\sqrt{s}$ = 22.5 ÷ 53.0 GeV (dash stripe) [5] and $\sqrt{s}$ = 6.84 GeV (P_L = 12 GeV/c) [9] (●). Theoretical curves : solid - $\sqrt{s}$ = 6.84 GeV, dash - $\sqrt{s}$ = 53 GeV.

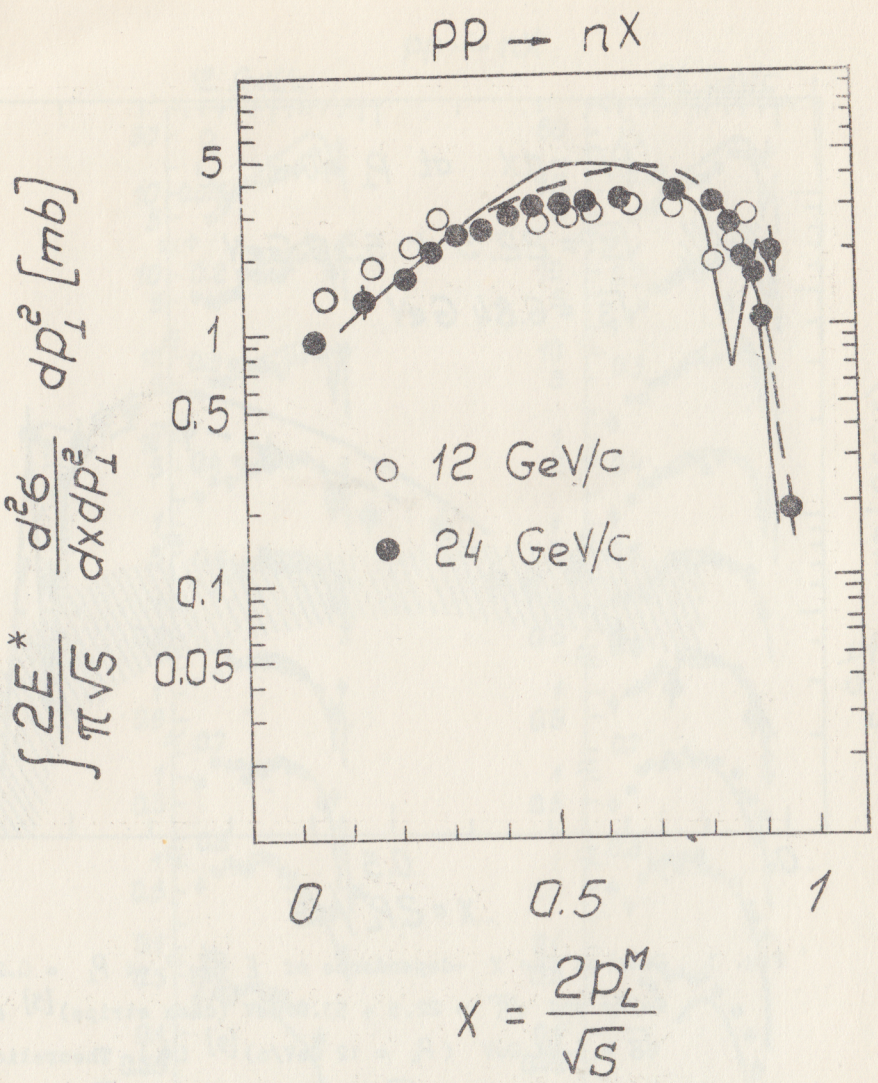


Fig. 4 Dependence of $\int \frac{2E^*}{\pi\sqrt{s}} \frac{d^2\sigma}{dx\,dp_T^2}\, dp_T^2$ on x [9] at p_L = 12 GeV/c (ϕ) and p_L = 24 GeV/c (ϕ). The solid curve is calculated at p_L = 12 GeV/c, the dotted one – at p_L = 24 GeV/c.

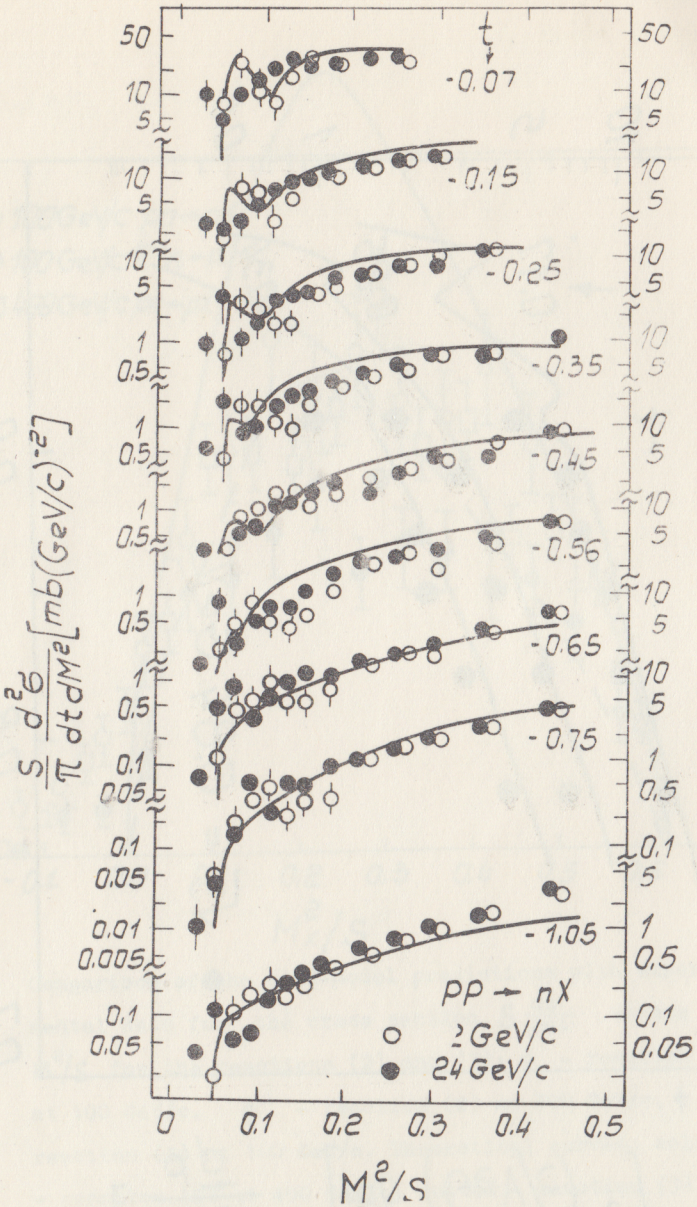


Fig. 5 $\frac{S}{\pi} \frac{d^2\sigma}{dt\,dM^2}$ versus M^2/S at momenta 12 (ϕ) and 24 (ϕ) GeV/c and fixed t for the reaction (1). The theoretical curve is calculated at p_L = 24 GeV/c.

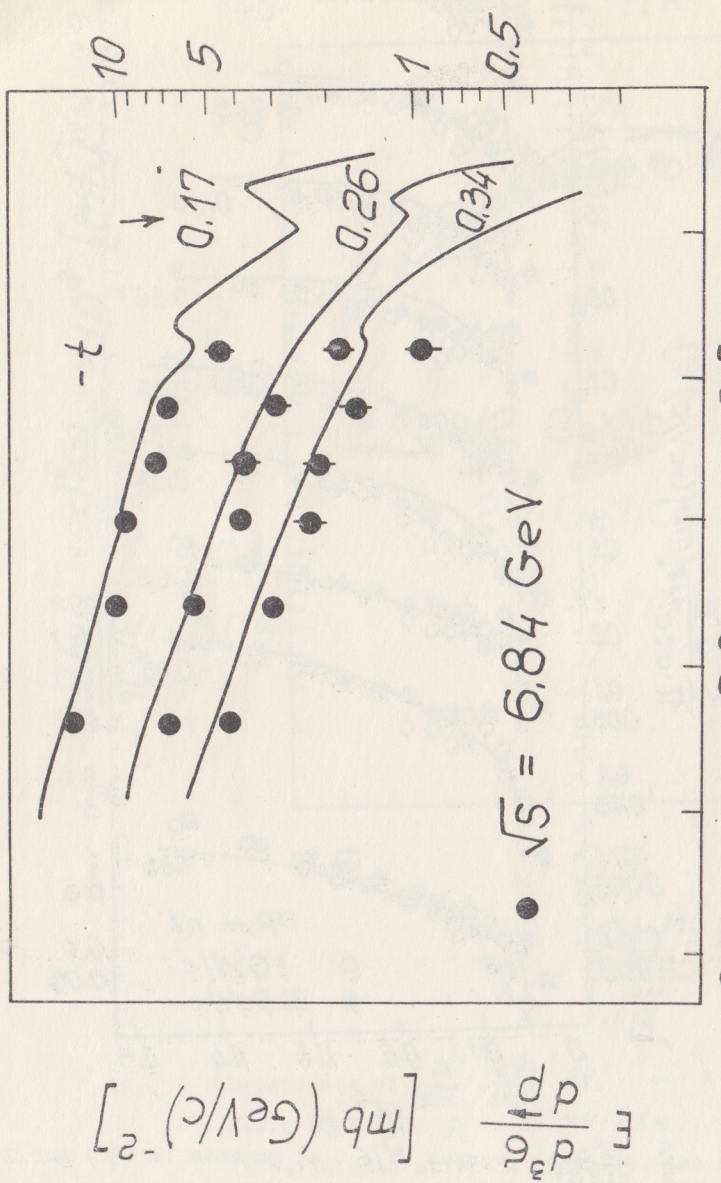


Fig. 6 Comparison of theoretical calculations and experimental data on the dependence of $E\frac{d\sigma}{d^3p}$ on $X = 1 - M^2/S$ for the reaction (1) at $\sqrt{S}$ = 6.84 GeV and fixed t [9]

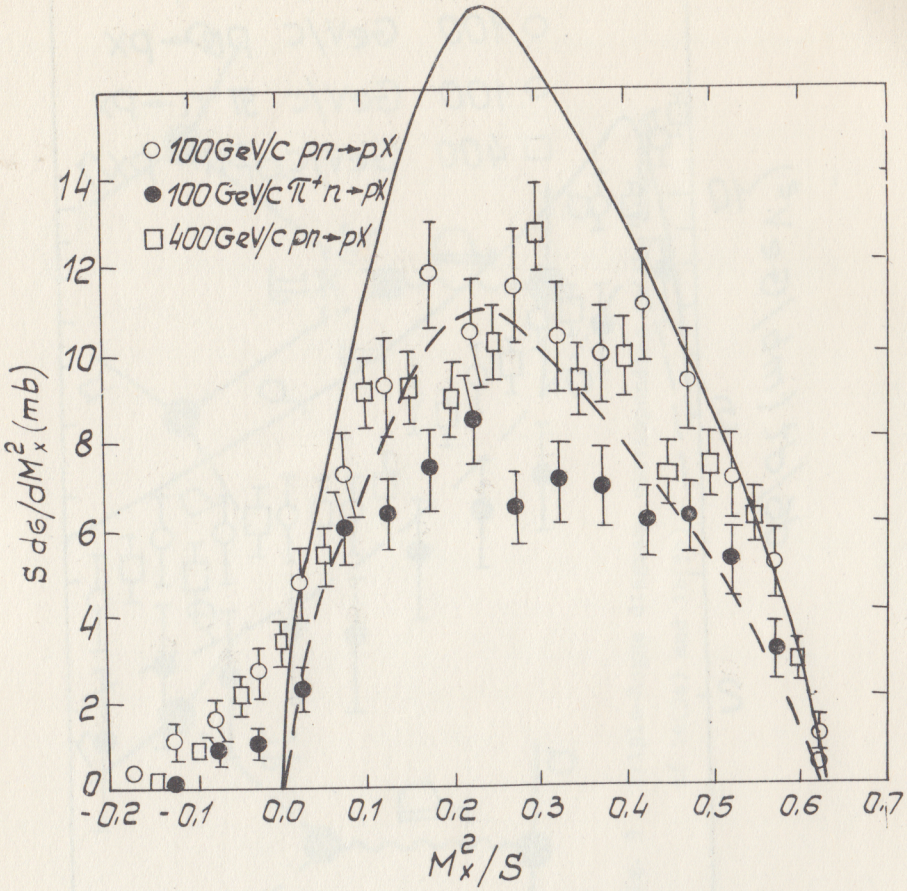


Fig. 7 Comparison of the OPER-model predictions with experimental data for the cross section $S\frac{d\sigma}{dM^2}$ versus M^2/S for the reactions (2) and (3): ϕ - reaction (2) at 100 GeV/c, ϕ - reaction (2) at 400 GeV/c, ϕ - reaction (3) at 100 GeV/c. Theoretical curves: solid - reaction (2) at 400 GeV/c, dotted - reaction (3) at 100 GeV/c.

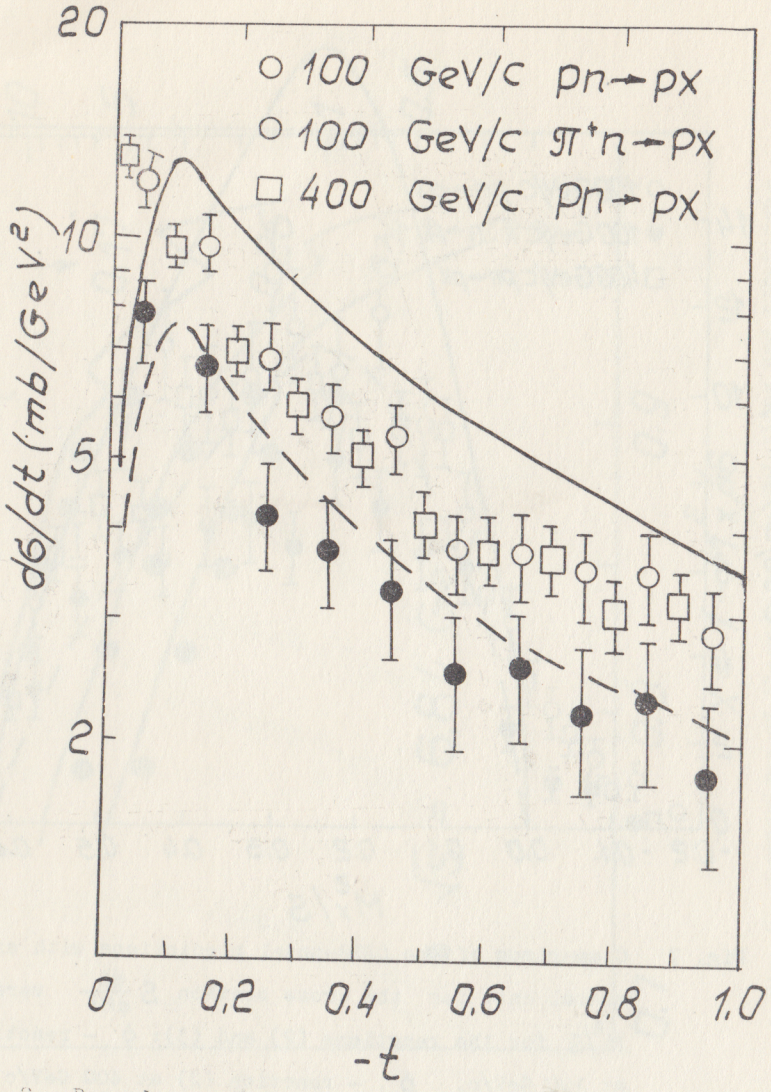


Fig. 8 Dependence of the cross section $d\sigma/dt$ on t for the reactions (2) and (3). The same symbols are used as in Fig. 7.

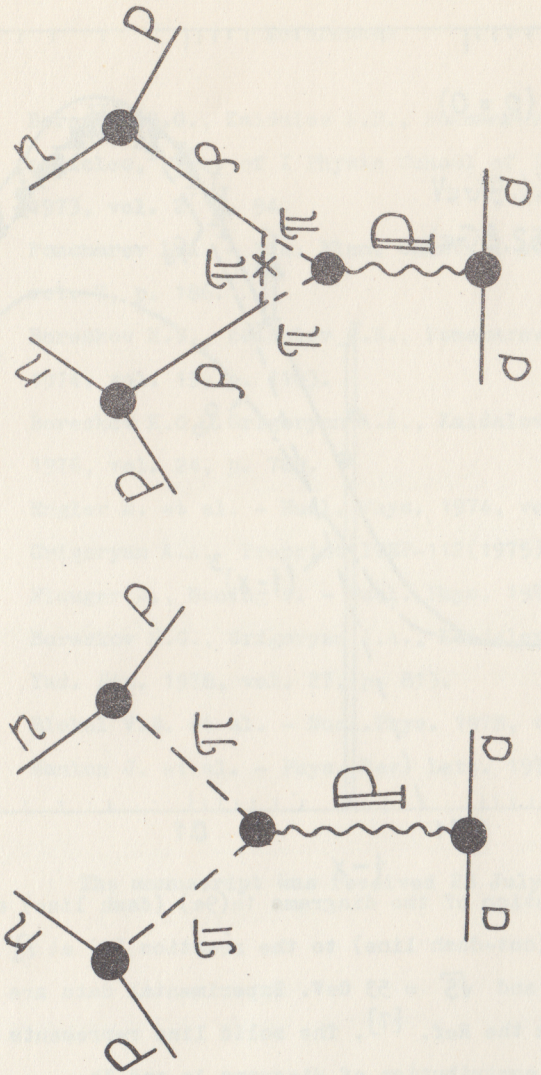


Fig. 9 Triple-Regge diagrams corresponding to the diagrams of 1a(9a) and 1b(9b).

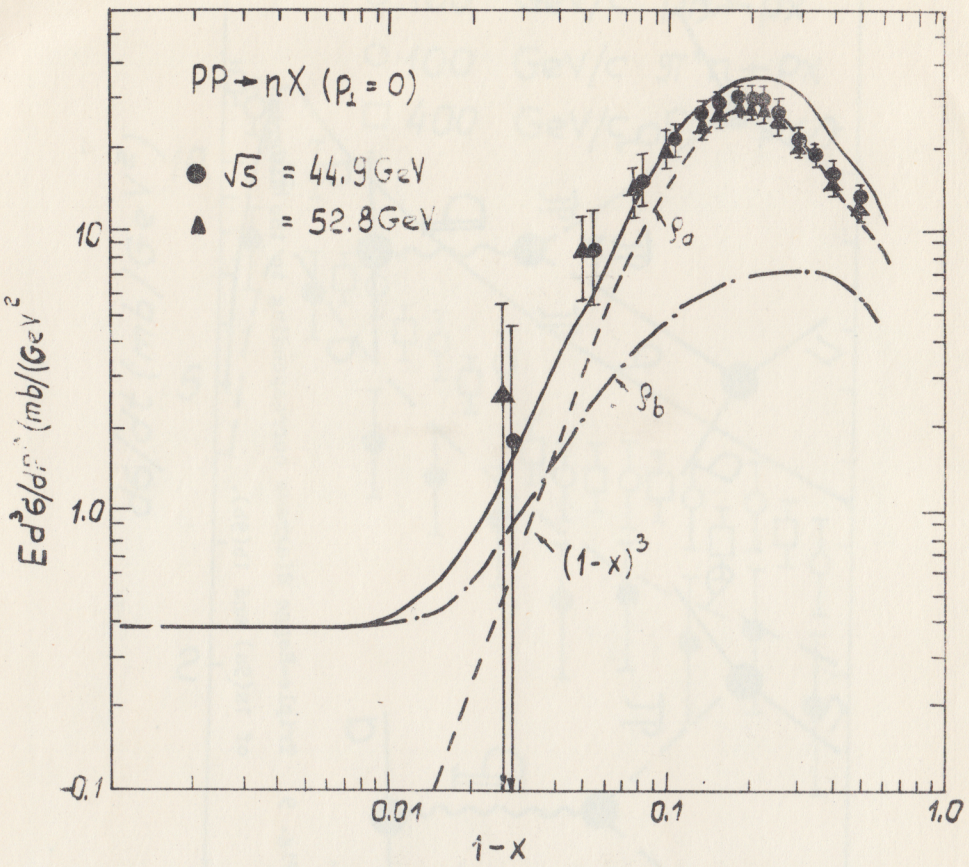


Fig. 10 Contribution of the diagrams 1a(9a) (dash line) and 1b(9b) (dot-dash line) to the reaction (1) at $P_\perp$ = 0 GeV/c and $\sqrt{s}$ = 53 GeV. Experimental data are taken from the Ref. [7]. The solid line represents the summary contribution of diagrams 1a and 1b.

References

1. Boreskov K.G., Kaidalov A.B., Ponomarev L.A. Elementary particles, Proc. of I Physic School of ITEP, M., "Atomizdat" 1973, vol. 2, p. 94.
2. Ponomarev L.A. - Fiz. Elem. Chast. i Atom. Yadra, 1976, vol. 7, p. 186.
3. Boreskov K.G., Kaidalov A.B., Ponomarev L.A. - Yad. Fiz., 1974, vol. 19, p. 1103.
4. Boreskov K.G., Grigoryan A.A., Kaidalov A.B. - Yad. Fiz., 1976, vol. 24, p. 789.
5. Engler A. et al. - Nucl. Phys. 1974, vol. B84, p. 565.
6. Grigoryan A.A. Preprint ITEP-112(1975).
7. Flauger W., Moning F. - Nucl. Phys. 1976, vol. B109, p.347.
8. Boreskov K.G., Grigoryan A.A., Kaidalov A.B., Levintov I.I. Yad. Fiz. 1978, vol. 27, p. 813.
9. Blobel V.B. et al. - Nucl.Phys. 1978, vol. B135,.p.379.
10. Hanlon J. et al. - Phys. Rev. Lett. 1976, vol. 37, p. 967.

The manuscript was received 28 July 1981.

Г.Г.АРАКЕЛЯН, А.А.ГРИГОРЯН

ИНКЛЮЗИВНЫЕ РЕАКЦИИ С ПЕРЕЗАРЯДКОЙ НУКЛОНОВ
И МОДЕЛЬ OPER

(на английском языке, перевод Л.Н.Багдасаряна)

Ереванский физический институт

Тех.редактор А.С.Абрамян

Заказ562 ВФ-05558 Тираж 299

Препринт ЕФИ Формат издания 60x84/16
Подписано к печати II/XI-8I I,5 уч.изд.л. Ц. I0 к.

Издано Отделом научно-технической информации
Ереванского физического института, Ереван-36,пер.Маркаряна 2